JGP Journal of General Physiology

VIEWPOINT

The ins and outs of vesicular monoamine transporters

Dana Yaffe[1], Lucy R. Forrest[2], and Shimon Schuldiner[1]

The H^+-coupled vesicular monoamine transporter (VMAT) is a transporter essential for life. VMAT mediates packaging of the monoamines serotonin, dopamine, norepinephrine, and histamine from the neuronal cytoplasm into presynaptic vesicles, which is a key step in the regulated release of neurotransmitters. However, a detailed understanding of the mechanism of VMAT function has been limited by the lack of availability of high-resolution structural data. In recent years, a series of studies guided by homology models has revealed significant insights into VMAT function, identifying residues that contribute to the binding site and to specific steps in the transport cycle. Moreover, to characterize the conformational transitions that occur upon binding of the substrate and coupling ion, we have taken advantage of the unique and powerful pharmacology of VMAT as well as of mutants that affect the conformational equilibrium of the protein and shift it toward defined conformations. This has allowed us to identify an important role for the proton gradient in driving a shift from lumen-facing to cytoplasm-facing conformations.

Introduction

Classical synaptic transmission involves the release of the neurotransmitter from the presynaptic cell into the synaptic cleft, where it interacts with receptors on the postsynaptic cell, leading to signal transduction. In most cases, termination of the signal is achieved by active removal of the neurotransmitter from the synaptic cleft by sodium-coupled transporters located on the cell membrane (Torres and Amara, 2007; Kristensen et al., 2011). Subsequently, vesicular neurotransmitter transporters remove the neurotransmitter from the cytoplasm and store it in secretory vesicles (Buchanan et al., 1976; Gorga and Lienhard, 1981; Johnson, 1988; Schuldiner et al., 1995; Weihe and Eiden, 2000; Edwards, 2007; Jacobs et al., 2007; Bulling et al., 2012). The storage of monoamines (serotonin, dopamine, histamine, adrenaline, and noradrenaline) is performed by the vesicular monoamine transporters (VMATs) 1 and 2. VMATs catalyze active removal of amines from the cytosol into the storage vesicles, coupled to the movement of two protons in the opposite direction. They therefore depend on the proton electrochemical gradient generated by the vesicular H^+-ATPase (Johnson, 1988; Schuldiner et al., 1995; Weihe and Eiden, 2000; Eiden et al., 2004; Anne and Gasnier, 2014).

VMAT1 and VMAT2 differ in expression pattern and in affinity toward the various substrates. Although some species-dependent variations may exist in the expression of the VMAT isoforms, human VMAT2 expresses mostly in neurons, whereas human VMAT1 is found in neuroendocrine cells. VMAT2 displays a higher affinity toward the diverse substrates and is the only isoform capable of transporting histamine (Peter et al., 1994; Erickson et al., 1996). In addition to the endogenous substrates, nonnatural substrates include the neurotoxin *N*-methyl-4-phenylpyridinium (MPP^+; Liu et al., 1992a,b) and acriflavine (Gros and Schuldiner, 2010).

The pharmacology of vesicular amine transport differs from that of plasma membrane amine transport with high affinity inhibition by reserpine and tetrabenazine but not by cocaine or antidepressants (Torres and Amara, 2007; Kristensen et al., 2011). Reserpine is an indole alkaloid, antipsychotic, and antihypertensive drug. The clinical use of reserpine has diminished over time, and it is now used mainly in veterinary medicine (Stitzel, 1976; Fraser, 1996; but also see Nur and Adams, 2016). Nevertheless, the discovery of reserpine enabled several important lines of scientific inquiry, including the mechanism of dopamine storage and release in the central nervous system as well as the generation of animal models of Parkinsonism. Tetrabenazine, on the other hand, is used for the symptomatic treatment of hyperkinetic disorders associated with Huntington's disease and Tourette's syndrome (Kenney and Jankovic, 2006).

Reserpine is a high-affinity (Deupree and Weaver, 1984; Scherman and Henry, 1984) competitive inhibitor (Jonasson et al., 1964; Kanner et al., 1979). Detailed analysis of the binding process revealed that reserpine binding has a unique profile because it is accelerated by the proton gradient, suggesting that translocation of at least one proton is needed to expose the high-affinity binding site (Weaver and Deupree, 1982; Scherman and Henry, 1984; Rudnick et al., 1990; Stern-Bach et al., 1990).

[1]Department of Biological Chemistry, Alexander Silberman Institute of Life Sciences, Hebrew University, Jerusalem, Israel; [2]Computational Structural Biology Section, National Institute of Neurological Disorders and Stroke, National Institutes of Health, Bethesda, MD.

Correspondence to Shimon Schuldiner: shimon.schuldiner@huji.ac.il; Dana Yaffe: dana.yaffe@mail.huji.ac.il; Lucy R. Forrest: lucy.forrest@nih.gov.

In contrast with reserpine, tetrabenazine is a noncompetitive inhibitor of VMAT2. Tetrabenazine is only a very weak inhibitor of VMAT1 (Peter et al., 1994) and as a result predominantly depletes central rather than peripheral amine stores (Carlsson, 1966). For tetrabenazine inhibition of VMAT2, a general mechanism has been proposed that involves two distinct steps, namely that initial tetrabenazine binding triggers a conformational change resulting in a dead-end complex of tetrabenazine with the transporter. According to this proposed mechanism, binding may be low affinity in the initial stage; tight binding and transport inhibition will be observed only when the conformational change has occurred (Ugolev et al., 2013).

The VMATs are members of the SLC18 human solute carrier family, which also includes the vesicular acetylcholine transporter (Anne and Gasnier, 2014) and the recently identified vesicular polyamine transporter (Hiasa et al., 2014). The SLC18 family is part of the major facilitator superfamily (MFS), the largest family of secondary active membrane transporters, whose members transport a diverse range of substrates (Saier et al., 1999). Members of this family are ubiquitous in all kingdoms of life, from bacteria to higher eukaryotes. Mechanistically, this family of transporters includes antiporters, symporters, and uniporters (Paulsen et al., 1996; Law et al., 2008) that are classified into a large number of subfamilies (Pao et al., 1998). Sequence motifs have been identified in transmembrane (TM) helices 1, 2, 7, and 8 in all MFS transporters, presumably reflecting their overall fold and function (Paulsen et al., 1996). Additional sequence motifs, namely RxxxGxG in TM4, GxxxGPxxG in TM5, and AxxxMSxxAG in TM11, are common to an MFS subfamily referred to as the drug/antiporter family number 1 (DHA-1, formerly DHA-12; tcdb family 2.A.1.2; Paulsen et al., 1996; Vardy et al., 2005). The DHA-1 subfamily includes VMAT and the other members of the SLC18 family, along with prokaryotic transporters, such as the *Escherichia coli* proteins MdfA, MdtM, and EmrAB, which confer bacterial cells with resistance to a range of different drugs (Pao et al., 1998). The relationships indicated by this phylogenetic analysis are consistent with the aforementioned pharmacological profile of VMAT, which resembles that of bacterial multidrug transporters (Yelin and Schuldiner, 1995). Indeed, using yeast genetics, it was demonstrated that three mutations suffice to transform rat VMAT2 into a multidrug transporter (Gros and Schuldiner, 2010); these mutations cause rat VMAT2 to lose the ability to transport neurotransmitters while still conferring resistance against the toxic substrates MPP, ethidium, and acriflavine.

Early work predicted that almost all MFS proteins are arranged in 12 TM α-helices (Law et al., 2008), and later structural analysis substantiated that prediction (Yan, 2015). A weak, yet clear, sequence similarity between the N-terminal (TM helices 1–6) and the C-terminal (TM helices 7–12) halves of a given MFS protein suggests that this architecture may have arisen because of a gene duplication and fusion event (Law et al., 2008). In recent years, MFS transporters have been the subject of many structural studies, and we are currently witnessing a remarkable increase in available structures; as of February 2018, there are 63 structures (of 23 unique proteins) in MemProtMD (a database for membrane proteins of known structure; http://memprotmd.bioch.ox.ac.uk), representing many diverse families. Analysis of the structures concluded that the two aforementioned halves (N terminal and C terminal) each form a bundle of helices that are related by twofold pseudosymmetry with an axis that runs normal to the membrane and between the two halves (Forrest, 2015; Yan, 2015). Further analysis revealed the presence of inverted topology repeat units within each of the domains (Hirai et al., 2002; Radestock and Forrest, 2011). That is, the first three helices (repeat unit A) are related in structure to the second three helices (repeat unit B) via a pseudo-twofold symmetry axis that runs through the center of the six-TM domain and parallel with the membrane plane (Fig. 1). A similar relationship is found for the two pairs of three TM helices in the C-terminal domain (repeat units C and D).

For more than 50 years now, the working model of substrate transport has been the alternating access mechanism (Mitchell, 1957; Jardetzky, 1966). According to this mechanism, one binding site can be alternately exposed by a conformational change to either side of the membrane (Jardetzky, 1966; Forrest and Rudnick, 2009). In the case of an antiporter such as VMAT, the conformational change occurs only when substrate or one or more protons are bound, and not when the binding site is empty. Biochemical evidence and the assortment of crystal structures from the MFS members solved in various conformations representing different steps in the transport cycle support the alternating state mechanism of transport (Forrest et al., 2011; Kaback, 2015; Yan, 2015). Notably, it has been proposed that the alternating access mechanism in the MFS family, as well as in other secondary active transporter families such as the neurotransmitter: sodium symporters and the excitatory amino acid transporters, arises from exchanging conformations of inverted-topology repeats (Forrest et al., 2008; Crisman et al., 2009; Forrest and Rudnick, 2009; Radestock and Forrest, 2011).

To preclude dissociation of either substrates or protons while the protein reorients, permeability barriers, referred to loosely as "gates," must prevent the formation of a continuous open pathway that would function as an uncoupled substrate or proton channel. An expected intermediate, therefore, is a fully occluded state, closed on both sides, formed by the flexing of TM helices around the bound substrate(s) with "hinge points" on either side of the cavity at the interface between the two halves of the transporter. Structures of fully occluded conformations of MFS transporters are rare, suggesting that this state is transient and metastable, consistent with the requirement that the transporter exchange stochastically between end states when the substrates are bound. For VMAT, however, the question remains which components of the sequence contribute to the gates and hinge points during the transport of substrates.

Here, we review structure-guided studies that have provided insight into the nature of the gates and hinge points in VMAT and their role in the mechanism of proton-monoamine antiport, and we discuss a model describing the transport cycle of VMAT as an example for proton-coupled antiporters.

Homology modeling

Despite the considerable increase in the number of available crystal structures of MFS transporters, obtaining a diffracting crystal

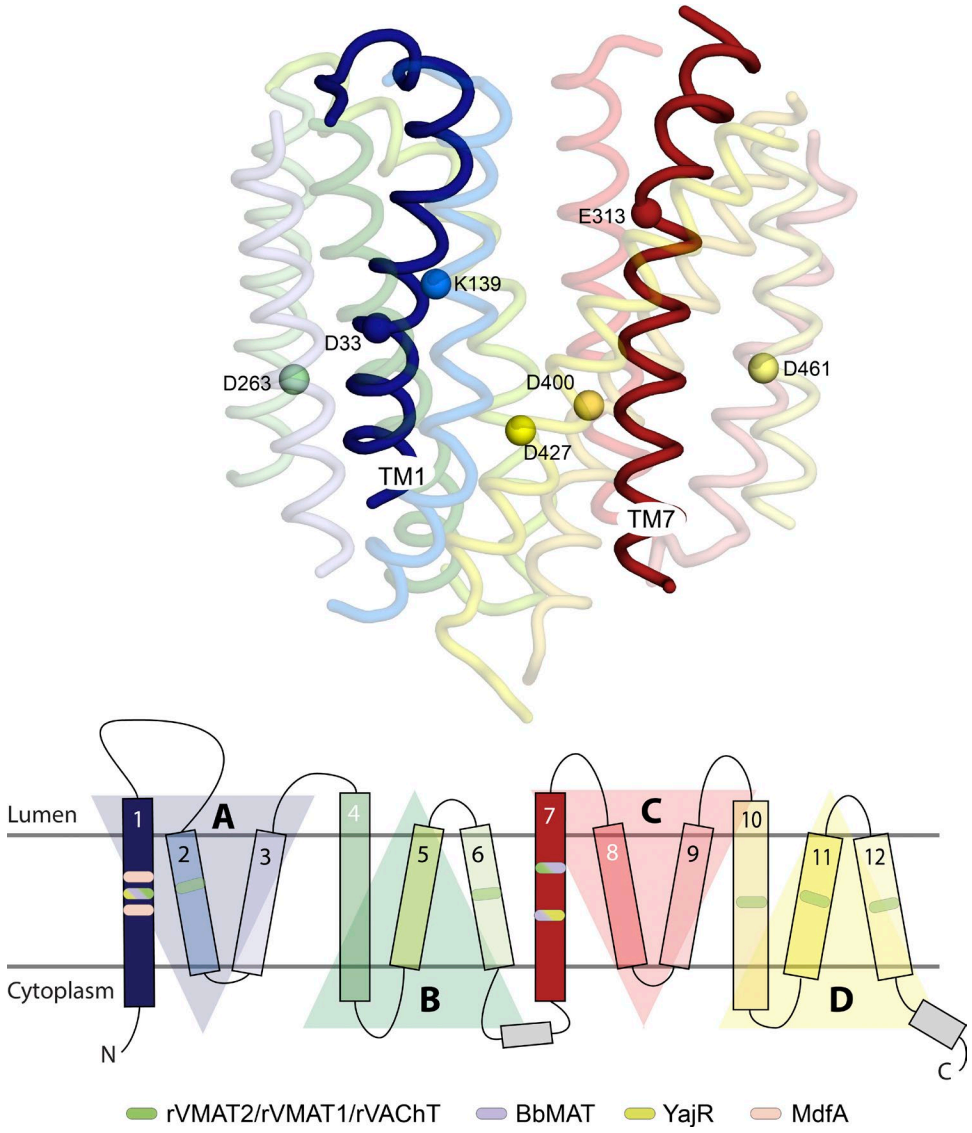

Figure 1. **Membrane-embedded charged residues in VMAT2.** Top: Structural model of rVMAT2 in the lumen-facing conformation (C_{lum}'), indicating the position of membrane-embedded charged residues in rVMAT2 (spheres) and colored according to TM helix, with the N-terminal half in shades of blue and green, and the C-terminal half in shades of red and yellow. Bottom: TM topology of antiporters from the DHA-1 family, colored according to the structure figure above. The structure of YajR (Protein Data Bank accession no. 3WDO) and the homology model of BbMAT were aligned to identify the conserved membrane-embedded charged residues, which are indicated as ellipses, based on the color coding indicated in the legend. Transparent triangles indicate the location of three-helix structural repeats in the N-terminal (blue and green) and C-terminal halves (pink and yellow) of the MFS fold.

of a eukaryotic protein and, more specifically, a mammalian protein remains a major challenge. Currently, the glucose (GLUT1/3) and fructose (GLUT5) transporter are the only mammalian MFS transporters for which structures have been reported (Deng et al., 2014, 2015; Nomura et al., 2015). Thus, a crystal structure of any vesicular neurotransmitter transporter is still lacking. Nevertheless, in recent years, several factors have enabled the development of reasonable structural models of vesicular neurotransmitter transporters. The reliability of a homology model depends on three key factors: first, the availability of a high-resolution structure of a protein with a similar sequence (a template); second, the degree of similarity between their sequences; and third, the accuracy of the alignment between the sequences of the template and the protein of interest. Thus, the availability of more crystal structures of transporters in different conformations has improved the potential accuracy of models of related proteins. Further advancements in the quality of sequence alignments have also been made possible by the availability of greater numbers of homologous sequences, as well as by developments in leveraging diverse structural and sequence information. A major challenge has long been that, by construction, homology modeling results in a model in a conformation identical to that of the template. This is somewhat limiting, because models of different conformations help predict the likely conformational change during the transport cycle. A breakthrough in the modeling of alternate conformations came from the understanding that by homology modeling of inverted-topology repeat units onto one another and thus swapping their conformations, it is possible to

Table 1. **Available structural models of VMATs**

Name	PMDB code	Template	Identity	Conformation	ProQM score	Reference
			%			
C_{cyt}	N/A	LacY 1PV6	~12[a]	Cytoplasm facing	0.561	Vardy et al., 2004
C_{cyt}'	PM0078823	LacY 1PV7	~12	Cytoplasm facing	0.616	Yaffe et al., 2013
C_{lum}	PM0078824	LacY 1PV7-RSM	~12	Lumen facing	0.616	Yaffe et al., 2013
C_{lum}'	PM0080553	YajR 3WDO	~18	Lumen facing	0.717	Yaffe et al., 2016

Structural models of rat VMAT2 have been reported in two alternate conformations. Three of these are available from the Protein Model Database (PMDB; Castrignanò et al., 2006). The models were built using different x-ray structure templates and, in one case (C_{lum}), a repeat-swapped model as a template; the underlying sequence alignments also differ. Identity: the percentage of identical residues in the target and template sequences in the region of the target that was modeled. The structural quality of the models is estimated by the ProQM score, which takes values of 0 to 1, and where higher values indicate better consistency with known structures (Ray et al., 2010). For reference, the ProQM scores of the templates are 0.729 (Protein Data Bank accession no. 1PV7) and 0.741 (Protein Data Bank accession no. 3WDO). N/A, not applicable.
[a]For the C_{cyt} model, the sequence identity was estimated from a TMalign structural alignment of the model to its template.

generate models of previously unknown states of several transporters (Forrest, 2013), including for the lactose permease LacY, the prototypical MFS transporter (Radestock and Forrest, 2011).

For VMAT2, the first reported structural model (C_{cyt}; see Table 1) was generated using the crystal structure of LacY in the cytoplasm-facing conformation as a template (Vardy et al., 2004). This model predicted a structural role for residues in TM12 (D461 and F464), as well as contacts between K139 in TM2 and D427 in TM11 and between Y342 from TM8 and D400 from TM10. Later, a second generation model of the same state (C_{cyt}') was obtained by applying a more advanced homology modeling strategy (Yaffe et al., 2013). Specifically, the alignment of rVMAT2 to the structural template (LacY) was improved by including sequence homologues belonging to three different subfamilies for which representative structures were known (LacY, EmrD, and GlpT), in addition to homologues of rVMAT2. The use of a larger number of sequences from diverse subfamilies altered the alignment between the rVMAT2 and LacY sequences in four TM helices (including shifts of a helix turn for TMs 2, 3, 7, and 8). These changes resulted in matching of the aforementioned MFS and DHA-1 family motifs, including motifs in TMs 1 and 7 and in the loops between TMs 2 and 3 and TMs 8 and 9, which had not been matched in the earlier alignment (Vardy et al., 2004). It is therefore likely that the pore-lining helices 1, 2, 7, and 8 and the residues contributing to the substrate-binding cavity are significantly more reliable in the later model (C_{cyt}').

The sequence identity between VMAT2 and LacY in the alignments used to guide the model building is very low (~12%) for both C_{cyt} and C_{cyt}' models. This level of similarity corresponds to an expected accuracy of 1.5–3.5 Å in the backbone, assuming an optimal alignment (Forrest et al., 2008; Olivella et al., 2013). However, scores of the structural models themselves indicate that the updated alignment led to a more reliable model. Specifically, the ProQM score, which measures the degree to which a structural model is consistent with observations from known membrane protein structures, is significantly higher for C_{cyt}' than for C_{cyt} (Table 1). Indeed, based on predictions from the C_{cyt}' cytoplasm-facing model (Fig. 1), key residues that are essential for transport activity could be identified.

Membrane-embedded carboxyl residues

Charged residues have been found in the binding sites for substrates and/or protons in several transporters and H^+ pumps (Lanyi, 1993; Rastogi and Girvin, 1999; Muth and Schuldiner, 2000; Adler and Bibi, 2004; Adler et al., 2004; Schuldiner, 2014; Kaback, 2015). Given that all of VMAT's substrates are positively charged, we hypothesized that acidic residues would be essential and chose to study them in depth. Ultimately, we identified two essential residues: D33 in TM1 and E313 in the symmetric TM7 (Fig. 1). The C_{cyt}' model predicted that six carboxylic residues and a lysine are located in the TM segments of rat VMAT2 (Fig. 1). Of the six acidic residues, five had been partially characterized; of these, D263 (TM6) and D461 (TM12) are not essential for the transport process (Merickel et al., 1997) and will not be further discussed here. Analysis of D400 (TM10) in the VMAT1 isoform suggested a possible functional role after substrate binding (Steiner-Mordoch et al., 1996); both C_{cyt} and C_{cyt}' models predicted that D400 interacts with Y342 (TM8) via a hydrogen bond, and biochemical analysis of VMAT2 supported this predicted structural role (Yaffe et al., 2013). D427 (TM11) and K139 (TM2) were previously suggested to interact (Merickel et al., 1997); we extended this predicted interaction network and identified a role in conformational change, which is further discussed below (Yaffe et al., 2013). D33 (TM1) was found to be essential for transport activity and tetrabenazine binding, but not for reserpine binding (Merickel et al., 1995; Yaffe et al., 2016). Notably, the conservative mutant D33N can still bind reserpine, albeit to lower levels (Yaffe et al., 2016). E313, the sixth carboxyl residue, had not been studied before our work because topology predictions had positioned it in the lumenal loop (Schuldiner et al., 1995; Steiner-Mordoch et al., 1996; Merickel et al., 1997). In the C_{cyt}' homology model, E313 is exposed to the central cavity and is located about midway along TM7. Multiple sequence alignment of a set of rVMAT2 homologues revealed that E313 is fully conserved within the higher organisms and highly conserved in the bacterial homologues. Mutagenesis of E313, even with conservative replacements such as Gln or Asp, completely abolished activity: the mutated transporter lost the ability to bind tetrabenazine and transport serotonin (Yaffe et al., 2013).

A significant role for D33 and E313 also emerged from studies of a close bacterial homologue, the *Brevibacillus brevis* monoamine transporter (BbMAT; Yaffe et al., 2014). Homology modeling of BbMAT suggested that there are six charged residues in its TM helices (D25, R108, D128, E222, E229, and H346), though of these six, only two are highly conserved, D25 and E229, the equivalent residues to D33 and E313 in rVMAT2, respectively. Mutating each of the above six residues and assaying for substrate transport confirmed that only D25 and E229 are essential for activity. Although all of the replacements tested at positions 108, 128, 222, and 346 can still confer drug resistance, position 25 can only tolerate a conservative replacement that maintains the carboxyl group. Interestingly, and different from E313 in rVMAT2, the BbMAT mutant E229Q was still able to catalyze transport, albeit to lower levels, because of the presence of a nonconserved Glu at position 222, two turns away, which can partially compensate for the absence of E229 (Yaffe et al., 2014). These results demonstrate a tolerance across the DHA-1 subfamily for different locations of the negative charge. Similar findings were obtained for MdfA, a bacterial multidrug transporter from *E. coli* and a distant homologue of VMAT. MdfA has two carboxyl residues in TM1, and the transporter can use either one, suggesting a requirement for a carboxyl residue that can be at several positions in TM1 (Sigal et al., 2009). Moreover, insertion of a carboxyl at a third location could replace both of the native carboxyls, further illustrating the promiscuity of the position of the acidic residue. A similar plasticity was also reported for LmrP, another drug/proton antiporter from the MFS family (Nair et al., 2016). This flexibility in the location of the carboxyl residues supports the notion that the major cavity of MFS H^+ antiporters houses a common binding site for substrates and protons, as also suggested for antiporters from other families (Lu et al., 2013; Nishizawa et al., 2013; Waight et al., 2013; Schuldiner, 2014). The exact location of the carboxyl residues may be not crucial for polyspecific transporters as long as there are enough binding determinants in the cavity, the geometry is not constraining, and the environment appropriately tunes the pKa. Biochemical and structural studies with EmrE, a small multidrug resistance H^+-coupled multidrug antiporter, support a general mechanism for H^+-coupled antiporters whereby the substrate and the protons cannot bind simultaneously to the protein (Schuldiner, 2014) and the overlap of the binding site results in a direct competition for its occupancy. In other examples, the "competition" seems to be indirect and is most likely achieved by some kind of allosteric mechanism (Fluman et al., 2012; Tanaka et al., 2013; Eicher et al., 2014; Schuldiner, 2014). To ensure the feasibility of such a mechanism, regardless of their specific structures or mechanisms, these antiporters have evolved so that they are exquisitely tuned to function at the very constant cytoplasmic pH maintained by cells. If the pKa of the carboxyl group were too low, it would generate a protein that at physiological pH binds substrate but cannot couple the substrate flux to the proton gradient. If the pKa were too high (greater than the cytoplasmic pH), substrate binding would be inhibited, thereby limiting the activity at physiological intracellular pH levels (Schuldiner, 2014).

It is noteworthy that the closely related protein YajR, which also belongs to the DHA-1 subfamily and whose structure was used as a template for a later VMAT2 model (see below), contains Arg24 in TM1 at the position corresponding to D33 of VMAT2 (according to the C_{cyt}' model), whereas TM7 contains His225 close to the position of E313 in TM7 and equivalent to E222 in BbMAT. The substrate of YajR is still unknown, but arginine residues are found in similar regions of TM1 (Arg45) and TM7 (Arg269) in another MFS protein, the *E. coli* glycerol phosphate transporter, which exchanges glycerol phosphate and inorganic phosphate. Moreover, another anion exchanger, NarK, which is specific for nitrate and nitrite, contains evolutionarily conserved and functionally important positively charged residues positioned symmetrically in TM2 (Arg89) and TM8 (Arg305; Zheng et al., 2013). This pattern of basic residues therefore suggests that YajR transports anionic substrates and implies an important role for pseudosymmetrically positioned charged residues in the transport of substrates by diverse MFS transporters.

Conformational changes

As mentioned above, the alternating access mechanism posits two transporter conformations, each of which exposes a central binding site to one side or the other of the membrane, in addition to an intermediate conformation in which access from both sides is prevented (occluded or closed). In the case of antiporters such as VMAT, interconversion is controlled by substrate and by coupling ions, i.e., H^+, but is forbidden in the apo protein. The most challenging questions relating to this mechanism are how the interconversion is facilitated and identifying the detailed conformational dynamics. In the case of VMAT2, the availability of an arsenal of pharmacological tools has allowed a glimpse into these events.

In the MFS transporters, a coordinated movement of the two domains relative to one another in a so-called "rocker-switch" mechanism is believed to mediate alternating access. However, there is evidence for bending and straightening of individual helices during this process, presumably to allow transient formation of intermediate occluded states (Newstead, 2017). To allow for bending during the transport cycle, the helices should include "flexible" points (Drew and Boudker, 2016). In the case of rVMAT2, its unique pharmacological profile and the power of yeast genetics allowed identification of several structural elements that may play such a role.

Helix breakers

The frequency of glycine and proline residues in α helices of membrane proteins is higher than that in water-soluble proteins (Sansom and Weinstein, 2000; Reiersen and Rees, 2001; Gimpelev et al., 2004). Moreover, about one third of the conserved residues in membrane domains are proline and glycine, suggesting that they have important functional roles (Liu et al., 2002). Glycine and proline are both considered classical "helix breakers": the small size of glycine confers conformational flexibility, while the loss of hydrogen donor potential and the steric hindrance of its side chain prevent helix formation by proline (von Heijne, 1991; Li and Deber, 1992; Cordes et al., 2002). The role of glycine and proline in conformational changes in ion channels has been extensively studied (Tieleman et al., 2001; Elinder et al., 2007), and it was demonstrated that they can supply the flexibility needed during

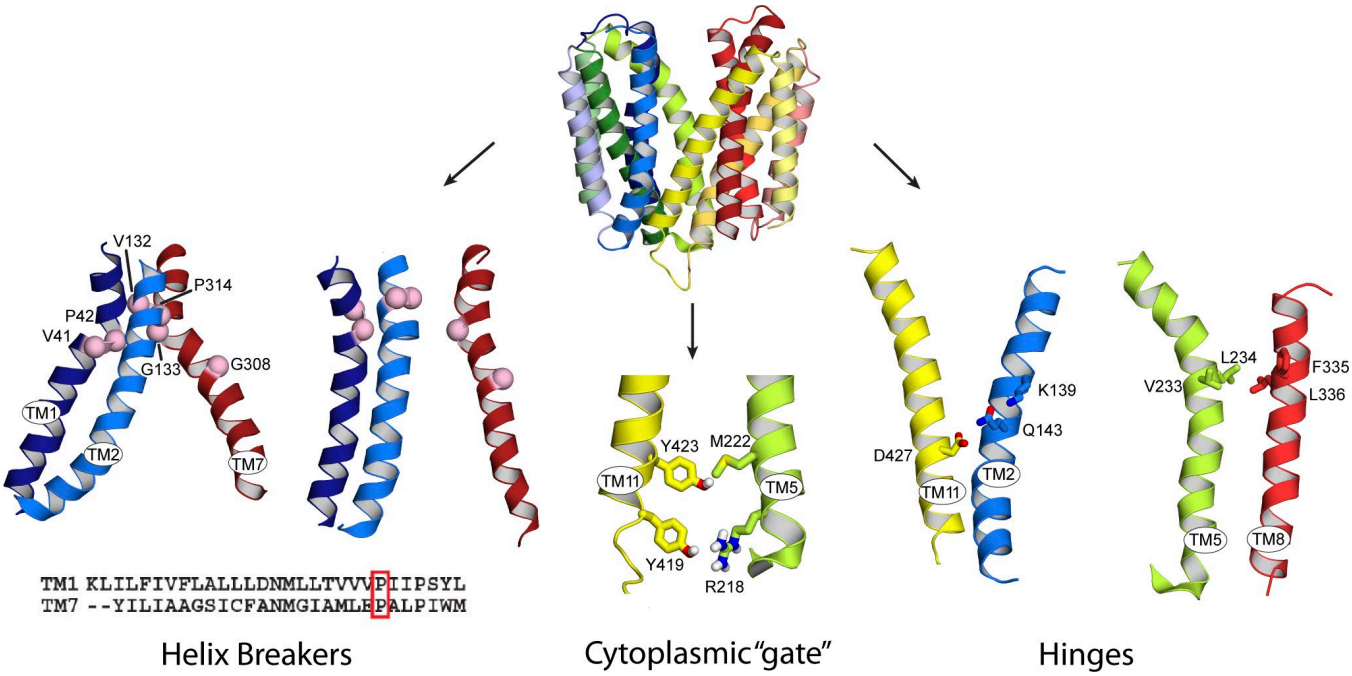

Figure 2. **Structural elements involved in conformational changes during the rVMAT2 transport cycle.** Top: Model of rVMAT2 in a lumen-facing state (C_{lum}') viewed along the plane of the membrane with the lumen at the top. Bottom left: Helix breakers. TM helices 1, 2, and 7 in the lumen-facing (left) and cytoplasm-facing (right) conformations are shown as cartoon helices, and relevant glycine and proline residues are indicated using pink spheres. Sequence alignment of helices 1 and 7. Helices were defined using the C_{lum}' model and aligned using ClustalW. Bottom middle: Gating residues. Magnification of the cytoplasmic domain of TM5 and TM11. Residues contributing to the cytoplasmic gate are shown as sticks. Bottom right: Hinges. Residues predicted to form interactions between TM2 and TM11 and between TM5 and TM8 in the vesicle lumen-facing conformation of rVMAT2 (sticks). These residues were predicted to form hinge points for the conformational change because the relative position of these residues is essentially unchanged between the cytoplasm and vesicle lumen-facing models. Adapted from Ugolev et al. (2013) and Yaffe et al. (2013, 2016).

channel gating. Glycine and proline were also found to be essential during conformational changes of transporters (Egenberger et al., 2012). For example, in the organic cation transporter 1 (Oct1), two glycine residues induce a helix break that is important for structural rearrangements during the transport cycle (Egenberger et al., 2012). Examples of proline residues involved in gating can be found in several MFS transporters, such as LacY, fucose permease, the peptide transporter, and the vesicular acetylcholine transporter (Weinglass et al., 2001; Chandrasekaran et al., 2006; Zhou et al., 2009; Sugihara et al., 2012; Newstead, 2015).

Expression of VMAT2 in *Saccharomyces cerevisiae* confers resistance to drugs such as the Parkinsonian toxin MPP^+, a substrate of VMAT2, because VMAT2 is targeted to the vacuolar membrane and sequesters MPP^+ from the cytoplasm into the vacuole (Gros and Schuldiner, 2010). The availability of this yeast expression system combined with the unique pharmacological profile of rVMAT2 enabled an unbiased random mutagenesis approach, which identified residues important for tetrabenazine inhibition (Ugolev et al., 2013). The nature of the screen allowed the isolation of mutants that exhibit decreased sensitivity to tetrabenazine, yet still support drug resistance. Remarkably, all of the identified mutations involved glycine, proline, or residues adjacent to conserved glycines or prolines, and they all cluster near the lumen end of the transporter (Fig. 2). The fact that these mutations alter the transporter's ability to bind tetrabenazine suggests that, at least in some cases, a local conformational change is needed for high-affinity binding.

A kinetic analysis revealed that some of the mutants (V41A, P42G, and P314G/L) have higher V_{max} values together with higher K_m values (similar K_{cat}). P314 is adjacent to E313, hinting at a possible local conformational change subsequent to substrate/proton binding. P42 (TM1) and P314 (TM7) both contribute to a highly conserved motif (with the sequence PxxP) in the MFS transporters (Paulsen et al., 1996; Vardy et al., 2005; Radestock and Forrest, 2011), and these positions are equivalent according to the pseudosymmetry between the N and C domains (Fig. 2). The strong conservation of these residues, together with the similarity of the effect of the mutations on transport kinetics, suggest a common role in the conformational equilibrium, as changes in kinetic properties may reflect a change in the rate-limiting step during the transport cycle. We suggest that the mutations reduce the ability of the protein to undergo a local conformational change needed for high-affinity binding of tetrabenazine and, at the same time, reduce the barrier of a rate-limiting step in the overall transport cycle, resulting in increased V_{max} values.

Hinges

As mentioned above, the major transport-associated conformational change requires a coordinated movement of the two domains around the substrate-binding site. In the case of the MFS fold, the two halves of the protein are expected to be in contact on either side of the central substrate cavity that will remain in contact during the cycle, around which the two bundles flex and straighten to open and close the two pathways. In this way, these

Table 2. **Residues positioned at interdomain hinge points in MFS structures**

MFS protein	Inward	Outward	TMs	Putative hinge residues
LacY	1PV7	5GXB	5–8	C148, W151, A155, T265, and E269
			2–11	S53, S56, Q60, C355, and Q359
XylE	4QIQ	4GC0[a]	5–8	I172, L176, and L326
			2–11	L65, I69, W416, and L417
GLUT5	4YBQ	4YBQ[b]	5–8	L167, T170, V325, and T328
			2–11	P78, G81, and W419
YajR	-	3WDO	5–8	V142, I146, M257, and F261
			2–11	Q65, S344, and T345

Structures of three MFS proteins in alternate conformations were compared to identify residues involved in contacts in both states at the hinge points connecting the two six-TM domains. The proteins compared were LacY or lactose permease, the xylose transporter XylE, and the glucose transporter GLUT5 from rat (Protein Data Bank accession no. 4YBQ) and bovine (Protein Data Bank accession no. 4YB9). YajR, the template for the most recent VMAT2 models, is included for reference.

[a]For XylE, one of the conformations is occluded.

[b]Residue numbering based on Protein Data Bank accession no. 4YBQ.

hinge points may mediate conformational changes while helping to retain the integrity of the overall transporter structure. Previous work suggested the existence of an ion pair between residues K139 (TM2) and D427 (TM11), each located in one of the two bundles, that may provide contact points during the movements (Merickel et al., 1997). However, the revised C_{cyt}' homology model predicted that these two residues were part of a larger network of hydrogen bonds between K139-Q143 (TM2) and D427 (TM11; Fig. 2). Model-guided mutagenesis supported the existence of this set of interactions connecting the two domains. Relocating the negative charge from helix 11 to helix 2 (Q143E–D427N) resulted in a fully active transporter, indicating the proximity of the two residues. Neutralizing the charge completely while maintaining the hydrophilic environment (K139Y–D427N) abolished transport activity, albeit while still allowing tetrabenazine binding, indicating that the deleterious effect on the transporter activity is not caused by improper folding. The approximate position of these residues and the observed effects on transport and binding together led to the suggestion that this set of interactions might function as a "hinge" during the conformational change of VMAT2 (Yaffe et al., 2013).

The K139–Q143–D427 interaction network connects the two domains on one side of the cavity through TM2 and TM11, raising the possibility of a second set of equivalent interactions at the interdomain contact point flanking the other side of the cavity, involving TM5 and TM8. Based on the MFS internal pseudosymmetry, a set of hydrophobic interactions were identified in the C_{cyt}' model involving residues V233 and L234 (TM5) and F335 and L336 (TM8).

Examining whether those interactions would remain formed during the conformational change required insight into the lumen-facing state. To this end, a structural model of rVMAT2 in that state, C_{lum}, was constructed based on a repeat-swapped model of LacY (Table 1; Yaffe et al., 2013). Although the overall expected accuracy of a model built on a model is likely to be lower than that of the structure-based models (i.e., a Cα position error >3.5 Å), it should be noted that the relative orientations of the helices were optimized to match those in the corresponding C_{cyt} models (Yaffe et al., 2013), and the ProQM score of the C_{lum} model is similar to that of C_{cyt} (Table 1). Therefore, comparison of the inward- and outward-facing models makes a reasonable prediction of the overall relative repositioning of those helices required to open or close the pathway. This comparison indicated that although TMs 2, 11, 5, and 8 may reorientate relative to one another, the abovementioned interaction networks are nevertheless predicted to remain connected. The data therefore suggest that these interactions supply contact points that, like hinges, mediate conformational changes of the two bundles. Analysis of different structures in the MFS family indicated that sets of favorable interactions, although not necessarily specific residues, connecting the domains are conserved within many different subfamilies (Yaffe et al., 2013). Recent studies have provided structures of individual MFS proteins in different conformations, including for LacY, XylE, and GLUT5 (Abramson et al., 2003; Sun et al., 2012; Jiang et al., 2013, 2016; Wisedchaisri et al., 2014; Nomura et al., 2015). In these structures, interactions involving clusters of either hydrophobic or hydrophilic residues are preserved in both conformations (Table 2), providing further support for the proposed hinge points between TM2 and TM11 and between TM5 and TM8 in VMAT2.

Gates

According to the alternating access mechanism, the transporter is never concurrently open to both sides, suggesting a requirement for flexible elements, sometimes called "gates," on both the cytoplasmic and luminal sides (Forrest et al., 2011). Considering the organization of the two bundles in MFS transporters, such gates should feature residues in the N and C domains that meet in some, but not all, of the conformations in the transport cycle. Indeed, gating residues have been identified in several MFS transporters (Ethayathulla et al., 2014; Deng et al., 2015; Fowler et al., 2015; Newstead, 2015; Taniguchi et al., 2015), often with the aid of crystal structures in different conformations. In the proton-coupled oligopeptide transporter family, for example, the cytoplasmic gate is formed by interactions between the cytoplasmic ends

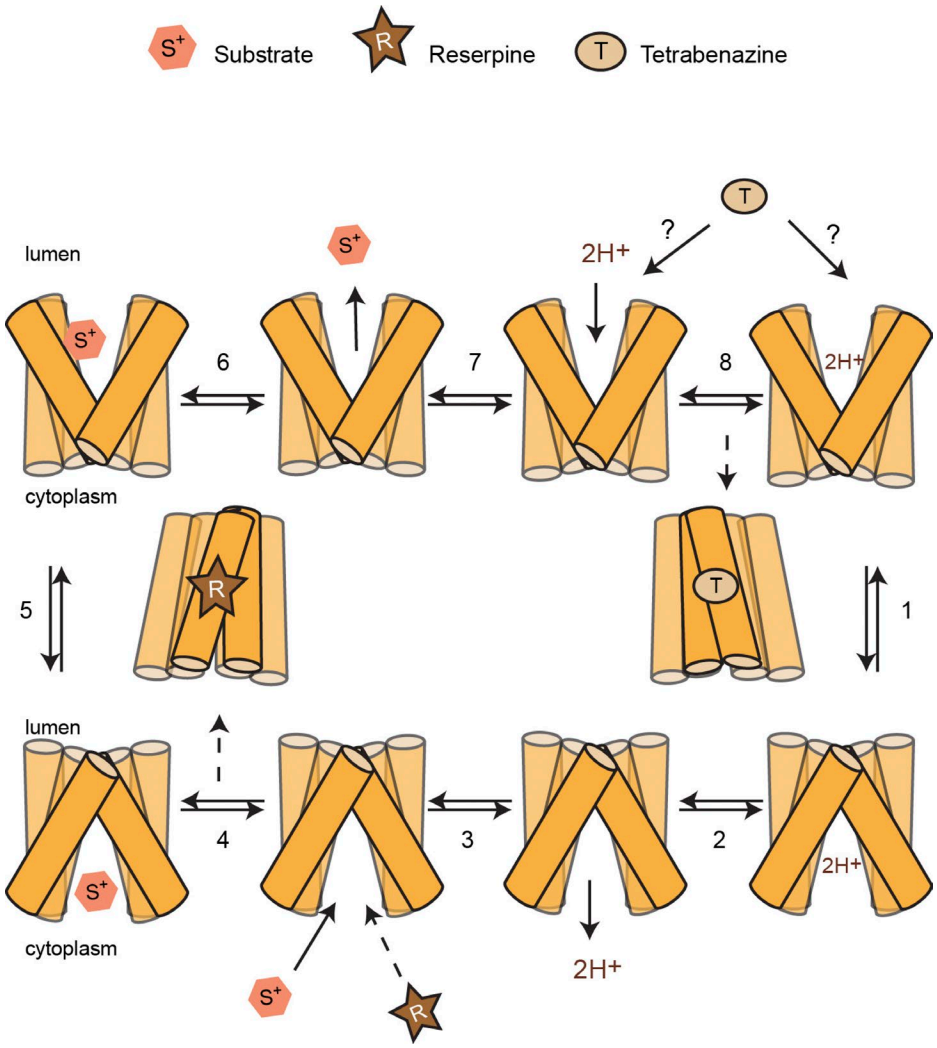

Figure 3. **Schematic of the proposed transport cycle.** For simplicity, only six TMs are shown. The cycle is assumed to involve eight steps (numbered). In the absence of a proton gradient, the dominant population is of the lumen-facing conformation, as indicated by the transporter's ability to bind tetrabenazine but not reserpine. Binding of protons enables the conformational switch to the cytoplasm-facing conformation (step 1), whereas binding of substrate enables the change to the lumen-facing conformation (step 5). Binding of tetrabenazine locks the transporter in a conformation that appears incompatible with substrate binding and is therefore presumably not cytoplasm facing (shown as an off-cycle state connected to step 8). Binding of reserpine also locks the transporter in a dead-end conformation, but reserpine binding competes with substrate binding, and therefore the reserpine-bound conformation is presumably cytoplasm facing (shown as an off-cycle state connected to step 4). The dashed arrow for reserpine indicates competition with substrate. Adapted from Yaffe et al. (2016).

of TM4 and TM5 as well as TM10 and TM11, and this gate closes upon binding of proton and substrate. In LacY, residues in TM1 and TM7 contribute to the periplasmic gate. After cross-linking double Cys replacements in these helices with homobifunctional reagents <15 Å in length, the mutants lose the ability to catalyze lactose transport. Strikingly, however, full or partial activity was observed when cross-linking was mediated by flexible reagents >15 Å in length. These results provide direct support for the argument that transport via LacY involves opening and closing of a large periplasmic cavity (Zhou et al., 2008), the opening of which provides the rate-limiting step for sugar binding (Smirnova et al., 2011). However, a more detailed understanding of the sequence of events leading to gate opening and closing is needed, especially for antiporters. Crystal structures, representing only a snapshot of the various conformational ensembles, are clearly essential but cannot fully explain the process as a whole.

In VMAT2, a unique pharmacological arsenal has enabled a better understanding of the role of the proton gradient and linked proton binding to a shift in the conformational equilibrium (Yaffe et al., 2016). Reserpine supplies information on the substrate binding site (Jonasson et al., 1964; Stitzel, 1976; Kanner et al., 1979; Darchen et al., 1989) and its accessibility because its binding is dramatically accelerated by the imposition of a proton gradient (Weaver and Deupree, 1982; Scherman and Henry, 1984; Rudnick et al., 1990), suggesting that the proton gradient facilitates a conformational change that exposes the substrate binding site to the cytoplasm. However, binding of tetrabenazine, a noncompetitive inhibitor of VMAT2, is independent of the proton gradient.

To predict interactions contributing to the cytoplasmic gate in rVMAT2, the model of the lumen-facing conformation was updated by using a more recent structure as a template, namely

that of *E. coli* YajR (Jiang et al., 2013). Despite only a relatively small increase in sequence identity, YajR is a significantly better template for VMAT2 than the LacY repeat-swapped model, as indicated by greater coverage in the alignment as well as a dramatic increase in the ProQM score to 0.717, close to that of known MFS structures (Table 1; Yaffe et al., 2016). The YajR-based lumen-facing model (Table 1, C_{lum}'), unlike its lower-resolution predecessor, predicts a set of interactions located at the cytoplasmic end of the transporter, connecting TM5 (R419 and M222) and TM11 (Y419 and Y423; Fig. 2). Mutating any of these four residues generated proteins that bind reserpine at fast rates, independent of the presence of a proton gradient, suggesting that in these mutants the reserpine binding site is constitutively accessible. Further characterization revealed that although mutants in position 222 or 423 can still bind tetrabenazine and transport serotonin, mutating residues Y419 and R218 abolishes both transport and tetrabenazine binding, but not reserpine binding. We therefore concluded that the interactions between TM5 and TM11 contribute to the cytoplasmic gate and are needed to maintain the equilibrium between the inward- and outward-facing conformations. Specifically, the interactions at the cytoplasmic gate stabilize the lumen (outward)-facing conformation, which appears to be the resting state conformation of the transporter at physiological pH. Weakening these interactions by mutagenesis shifts the conformational equilibrium and increases the fraction of VMAT2 in the cytoplasmic-facing conformation.

The results described above indicate that although mutants at positions 222 and 423 increase the likelihood that VMAT2 is in the cytoplasmic-facing conformation, they can still complete the catalytic cycle. However, interactions involving positions 218 and 419 seem to be essential for closing the cytoplasmic gate, as indicated by the fact that mutants at these positions do not transport and do not bind tetrabenazine.

Collectively, the results support the notion that reserpine and the substrate bind to the cytoplasmic-facing conformation, whereas tetrabenazine binds to the lumen-facing conformation in a noncompetitive fashion. The findings indicate that the two inhibitors demonstrate a conformational selectivity that, to our knowledge, has thus far only been reported for three other transporters, namely the ATP–ADP carrier, the human erythrocyte glucose transporter, and the serotonin transporter (Buchanan et al., 1976; Gorga and Lienhard, 1981; Jacobs et al., 2007; Bulling et al., 2012).

Proposed transport cycle

Incorporating all of our data, we have proposed a model describing the transport cycle of VMAT as an example for proton-coupled antiporters (Fig. 3). In the absence of a proton gradient, at physiological pH, the "resting" conformation of the apo transporter is the lumen-facing conformation, and the transition to the cytoplasm-facing conformation is extremely slow, as indicated by the hours needed to bind reserpine. Acidification of the lumen affects the protonation of two key residues (D33 in TM1 and E313 in TM7), which facilitates a chain of events including opening of the cytoplasmic gate, thereby enabling the conformational transition and increasing the fraction of protein in the cytoplasm-facing conformation (Fig. 3, step 1). Proton release to the more alkaline side of the membrane increases the affinity of the binding site to either substrate or reserpine. Substrate binding induces a second conformational change to the lumen-facing conformation, allowing for substrate release (Fig. 3, step 5). This lumen-facing conformation also exposes the binding site for tetrabenazine, whose binding creates a dead-end conformation.

Future perspectives

Although these studies have provided important insights into the mechanism of proton-monoamine antiport by VMATs, many questions still remain, particularly relating to binding sites of the many substrates and inhibitors and the conformational changes connecting the two end states. We anticipate that addressing these questions will require improved models or structural data for conformations such as the occluded and ligand-bound states, complemented by spectroscopy, biochemistry, and computer simulations, to uncover the conformational dynamics occurring during neurotransmitter storage into vesicles.

Acknowledgments

S. Schuldiner is Mathilda Marks-Kennedy Professor of Biochemistry at the Hebrew University of Jerusalem. This research was supported by National Institutes of Health grant NS16708, Israel Science Foundation grants 97/12 and 143/16, United States - Israel Binational Science Foundation grant 2013198 (to S. Schuldiner), and the Division of Intramural Research of the National Institute of Neurological Disorders and Stroke, National Institutes of Health (to L.R. Forrest). D. Yaffe was the recipient of a Professor Rahamimoff Travel Grant from the United States - Israel Binational Science Foundation.

The authors declare no competing financial interests.

Author contributions: D. Yaffe, L.R. Forrest, and S. Schuldiner wrote the manuscript.

Lesley C. Anson served as editor.

Submitted: 16 January 2018
Accepted: 26 March 2018

References

Abramson, J., I. Smirnova, V. Kasho, G. Verner, H.R. Kaback, and S. Iwata. 2003. Structure and mechanism of the lactose permease of Escherichia coli. *Science.* 301:610–615. https://doi.org/10.1126/science.1088196

Adler, J., and E. Bibi. 2004. Determinants of substrate recognition by the Escherichia coli multidrug transporter MdfA identified on both sides of the membrane. *J. Biol. Chem.* 279:8957–8965. https://doi.org/10.1074/jbc.M313422200

Adler, J., O. Lewinson, and E. Bibi. 2004. Role of a conserved membrane-embedded acidic residue in the multidrug transporter MdfA. *Biochemistry.* 43:518–525. https://doi.org/10.1021/bi035485t

Anne, C., and B. Gasnier. 2014. Vesicular neurotransmitter transporters: mechanistic aspects. *Curr. Top. Membr.* 73:149–174. https://doi.org/10.1016/B978-0-12-800223-0.00003-7

Buchanan, B.B., W. Eiermann, P. Riccio, H. Aquila, and M. Klingenberg. 1976. Antibody evidence for different conformational states of ADP, ATP translocator protein isolated from mitochondria. *Proc. Natl. Acad. Sci. USA.* 73:2280–2284. https://doi.org/10.1073/pnas.73.7.2280

Bulling, S., K. Schicker, Y.W. Zhang, T. Steinkellner, T. Stockner, C.W. Gruber, S. Boehm, M. Freissmuth, G. Rudnick, H.H. Sitte, and W. Sandtner.

2012. The mechanistic basis for noncompetitive ibogaine inhibition of serotonin and dopamine transporters. *J. Biol. Chem.* 287:18524–18534. https://doi.org/10.1074/jbc.M112.343681

Carlsson, A. 1966. Drugs which block the storage of 5-hydroxytryptamine and related amines. *In* 5-Hydroxytryptamine and Related Indolealkylamines. O. Eichler, and A. Farah, editors. Springer-Verlag, Berlin. 529–592. https://doi.org/10.1007/978-3-642-85467-5_11

Castrignanò, T., P.D. De Meo, D. Cozzetto, I.G. Talamo, and A. Tramontano. 2006. The PMDB Protein Model Database. *Nucleic Acids Res.* 34:D306–D309. https://doi.org/10.1093/nar/gkj105

Chandrasekaran, A., A.M. Ojeda, N.G. Kolmakova, and S.M. Parsons. 2006. Mutational and bioinformatics analysis of proline- and glycine-rich motifs in vesicular acetylcholine transporter. *J. Neurochem.* 98:1551–1559. https://doi.org/10.1111/j.1471-4159.2006.03975.x

Cordes, F.S., J.N. Bright, and M.S. Sansom. 2002. Proline-induced distortions of transmembrane helices. *J. Mol. Biol.* 323:951–960. https://doi.org/10.1016/S0022-2836(02)01006-9

Crisman, T.J., S. Qu, B.I. Kanner, and L.R. Forrest. 2009. Inward-facing conformation of glutamate transporters as revealed by their inverted-topology structural repeats. *Proc. Natl. Acad. Sci. USA.* 106:20752–20757. https://doi.org/10.1073/pnas.0908570106

Darchen, F., D. Scherman, and J.-P. Henry. 1989. Reserpine binding to chromaffin granules suggests the existence of two conformations of the monoamine transporter. *Biochemistry.* 28:1692–1697. https://doi.org/10.1021/bi00430a040

Deng, D., C. Xu, P. Sun, J. Wu, C. Yan, M. Hu, and N. Yan. 2014. Crystal structure of the human glucose transporter GLUT1. *Nature.* 510:121–125. https://doi.org/10.1038/nature13306

Deng, D., P. Sun, C. Yan, M. Ke, X. Jiang, L. Xiong, W. Ren, K. Hirata, M. Yamamoto, S. Fan, and N. Yan. 2015. Molecular basis of ligand recognition and transport by glucose transporters. *Nature.* 526:391–396. https://doi.org/10.1038/nature14655

Deupree, J.D., and J.A. Weaver. 1984. Identification and characterization of the catecholamine transporter in bovine chromaffin granules using [3H] reserpine. *J. Biol. Chem.* 259:10907–10912.

Drew, D., and O. Boudker. 2016. Shared Molecular Mechanisms of Membrane Transporters. *Annu. Rev. Biochem.* 85:543–572. https://doi.org/10.1146/annurev-biochem-060815-014520

Edwards, R.H. 2007. The neurotransmitter cycle and quantal size. *Neuron.* 55:835–858. https://doi.org/10.1016/j.neuron.2007.09.001

Egenberger, B., V. Gorboulev, T. Keller, D. Gorbunov, N. Gottlieb, D. Geiger, T.D. Mueller, and H. Koepsell. 2012. A substrate binding hinge domain is critical for transport-related structural changes of organic cation transporter 1. *J. Biol. Chem.* 287:31561–31573. https://doi.org/10.1074/jbc.M112.388793

Eicher, T., M.A. Seeger, C. Anselmi, W. Zhou, L. Brandstätter, F. Verrey, K. Diederichs, J.D. Faraldo-Gómez, and K.M. Pos. 2014. Coupling of remote alternating-access transport mechanisms for protons and substrates in the multidrug efflux pump AcrB. *eLife.* 3:03145. https://doi.org/10.7554/eLife.03145

Eiden, L.E., M.K. Schäfer, E. Weihe, and B. Schütz. 2004. The vesicular amine transporter family (SLC18): amine/proton antiporters required for vesicular accumulation and regulated exocytotic secretion of monoamines and acetylcholine. *Pflugers Arch.* 447:636–640. https://doi.org/10.1007/s00424-003-1100-5

Elinder, F., J. Nilsson, and P. Arhem. 2007. On the opening of voltage-gated ion channels. *Physiol. Behav.* 92:1–7. https://doi.org/10.1016/j.physbeh.2007.05.058

Erickson, J.D., M.K. Schafer, T.I. Bonner, L.E. Eiden, and E. Weihe. 1996. Distinct pharmacological properties and distribution in neurons and endocrine cells of two isoforms of the human vesicular monoamine transporter. *Proc. Natl. Acad. Sci. USA.* 93:5166–5171. https://doi.org/10.1073/pnas.93.10.5166

Ethayathulla, A.S., M.S. Yousef, A. Amin, G. Leblanc, H.R. Kaback, and L. Guan. 2014. Structure-based mechanism for Na(+)/melibiose symport by MelB. *Nat. Commun.* 5:3009. https://doi.org/10.1038/ncomms4009

Fluman, N., C.M. Ryan, J.P. Whitelegge, and E. Bibi. 2012. Dissection of mechanistic principles of a secondary multidrug efflux protein. *Mol. Cell.* 47:777–787. https://doi.org/10.1016/j.molcel.2012.06.018

Forrest, L.R. 2013. Structural biology. (Pseudo-)symmetrical transport. *Science.* 339:399–401. https://doi.org/10.1126/science.1228465

Forrest, L.R. 2015. Structural Symmetry in Membrane Proteins. *Annu. Rev. Biophys.* 44:311–337. https://doi.org/10.1146/annurev-biophys-051013-023008

Forrest, L.R., and G. Rudnick. 2009. The rocking bundle: a mechanism for ion-coupled solute flux by symmetrical transporters. *Physiology (Bethesda).* 24:377–386.

Forrest, L.R., Y.W. Zhang, M.T. Jacobs, J. Gesmonde, L. Xie, B.H. Honig, and G. Rudnick. 2008. Mechanism for alternating access in neurotransmitter transporters. *Proc. Natl. Acad. Sci. USA.* 105:10338–10343. https://doi.org/10.1073/pnas.0804659105

Forrest, L.R., R. Krämer, and C. Ziegler. 2011. The structural basis of secondary active transport mechanisms. *Biochim. Biophys. Acta.* 1807:167–188. https://doi.org/10.1016/j.bbabio.2010.10.014

Fowler, P.W., M. Orwick-Rydmark, S. Radestock, N. Solcan, P.M. Dijkman, J.A. Lyons, J. Kwok, M. Caffrey, A. Watts, L.R. Forrest, and S. Newstead. 2015. Gating topology of the proton-coupled oligopeptide symporters. *Structure.* 23:290–301. https://doi.org/10.1016/j.str.2014.12.012

Fraser, H.S. 1996. Reserpine: a tragic victim of myths, marketing, and fashionable prescribing. *Clin. Pharmacol. Ther.* 60:368–373. https://doi.org/10.1016/S0009-9236(96)90193-9

Gimpelev, M., L.R. Forrest, D. Murray, and B. Honig. 2004. Helical packing patterns in membrane and soluble proteins. *Biophys. J.* 87:4075–4086. https://doi.org/10.1529/biophysj.104.049288

Gorga, F.R., and G.E. Lienhard. 1981. Equilibria and kinetics of ligand binding to the human erythrocyte glucose transporter. Evidence for an alternating conformation model for transport. *Biochemistry.* 20:5108–5113. https://doi.org/10.1021/bi00521a003

Gros, Y., and S. Schuldiner. 2010. Directed evolution reveals hidden properties of VMAT, a neurotransmitter transporter. *J. Biol. Chem.* 285:5076–5084. https://doi.org/10.1074/jbc.M109.081216

Hiasa, M., T. Miyaji, Y. Haruna, T. Takeuchi, Y. Harada, S. Moriyama, A. Yamamoto, H. Omote, and Y. Moriyama. 2014. Identification of a mammalian vesicular polyamine transporter. *Sci. Rep.* 4:6836. https://doi.org/10.1038/srep06836

Hirai, T., J.A. Heymann, D. Shi, R. Sarker, P.C. Maloney, and S. Subramaniam. 2002. Three-dimensional structure of a bacterial oxalate transporter. *Nat. Struct. Biol.* 9:597–600.

Jacobs, M.T., Y.W. Zhang, S.D. Campbell, and G. Rudnick. 2007. Ibogaine, a noncompetitive inhibitor of serotonin transport, acts by stabilizing the cytoplasm-facing state of the transporter. *J. Biol. Chem.* 282:29441–29447. https://doi.org/10.1074/jbc.M704456200

Jardetzky, O. 1966. Simple allosteric model for membrane pumps. *Nature.* 211:969–970. https://doi.org/10.1038/211969a0

Jiang, D., Y. Zhao, X. Wang, J. Fan, J. Heng, X. Liu, W. Feng, X. Kang, B. Huang, J. Liu, and X.C. Zhang. 2013. Structure of the YajR transporter suggests a transport mechanism based on the conserved motif A. *Proc. Natl. Acad. Sci. USA.* 110:14664–14669. https://doi.org/10.1073/pnas.1308127110

Jiang, X., I. Smirnova, V. Kasho, J. Wu, K. Hirata, M. Ke, E. Pardon, J. Steyaert, N. Yan, and H.R. Kaback. 2016. Crystal structure of a LacY-nanobody complex in a periplasmic-open conformation. *Proc. Natl. Acad. Sci. USA.* 113:12420–12425. https://doi.org/10.1073/pnas.1615414113

Johnson, R.G. Jr. 1988. Accumulation of biological amines into chromaffin granules: a model for hormone and neurotransmitter transport. *Physiol. Rev.* 68:232–307. https://doi.org/10.1152/physrev.1988.68.1.232

Jonasson, J., E. Rosengren, and B. Waldeck. 1964. Effects of some pharmacologically active amines on the uptake of anylalkylamines by adrenal medullary granules. *Acta Physiol. Scand.* 60:136–140. https://doi.org/10.1111/j.1748-1716.1964.tb02876.x

Kaback, H.R. 2015. A chemiosmotic mechanism of symport. *Proc. Natl. Acad. Sci. USA.* 112:1259–1264. https://doi.org/10.1073/pnas.1419325112

Kanner, B.I., H. Fishkes, R. Maron, I. Sharon, and S. Schuldiner. 1979. Reserpine as a competitive and reversible inhibitor of the catecholamine transporter of bovine chromaffin granules. *FEBS Lett.* 100:175–178. https://doi.org/10.1016/0014-5793(79)81158-8

Kenney, C., and J. Jankovic. 2006. Tetrabenazine in the treatment of hyperkinetic movement disorders. *Expert Rev. Neurother.* 6:7–17. https://doi.org/10.1586/14737175.6.1.7

Kristensen, A.S., J. Andersen, T.N. Jørgensen, L. Sørensen, J. Eriksen, C.J. Loland, K. Strømgaard, and U. Gether. 2011. SLC6 neurotransmitter transporters: structure, function, and regulation. *Pharmacol. Rev.* 63:585–640. https://doi.org/10.1124/pr.108.000869

Lanyi, J.K. 1993. Proton translocation mechanism and energetics in the light-driven pump bacteriorhodopsin. *Biochim. Biophys. Acta.* 1183:241–261. https://doi.org/10.1016/0005-2728(93)90226-6

Law, C.J., P.C. Maloney, and D.N. Wang. 2008. Ins and outs of major facilitator superfamily antiporters. *Annu. Rev. Microbiol.* 62:289–305. https://doi.org/10.1146/annurev.micro.61.080706.093329

Li, S.C., and C.M. Deber. 1992. Influence of glycine residues on peptide conformation in membrane environments. *Int. J. Pept. Protein Res.* 40:243–248. https://doi.org/10.1111/j.1399-3011.1992.tb00297.x

Liu, Y., D. Peter, A. Roghani, S. Schuldiner, G.G. Privé, D. Eisenberg, N. Brecha, and R.H. Edwards. 1992a. A cDNA that suppresses MPP+ toxicity encodes a vesicular amine transporter. *Cell.* 70:539–551. https://doi.org/10.1016/0092-8674(92)90425-C

Liu, Y., A. Roghani, and R.H. Edwards. 1992b. Gene transfer of a reserpine-sensitive mechanism of resistance to N-methyl-4-phenylpyridinium. *Proc. Natl. Acad. Sci. USA.* 89:9074–9078. https://doi.org/10.1073/pnas.89.19.9074

Liu, Y., D.M. Engelman, and M. Gerstein. 2002. Genomic analysis of membrane protein families: abundance and conserved motifs. *Genome Biol.* 3:0054.

Lu, M., M. Radchenko, J. Symersky, R. Nie, and Y. Guo. 2013. Structural insights into H+-coupled multidrug extrusion by a MATE transporter. *Nat. Struct. Mol. Biol.* 20:1310–1317. https://doi.org/10.1038/nsmb.2687

Merickel, A., P. Rosandich, D. Peter, and R.H. Edwards. 1995. Identification of residues involved in substrate recognition by a vesicular monoamine transporter. *J. Biol. Chem.* 270:25798–25804. https://doi.org/10.1074/jbc.270.43.25798

Merickel, A., H.R. Kaback, and R.H. Edwards. 1997. Charged residues in transmembrane domains II and XI of a vesicular monoamine transporter form a charge pair that promotes high affinity substrate recognition. *J. Biol. Chem.* 272:5403–5408. https://doi.org/10.1074/jbc.272.9.5403

Mitchell, P. 1957. A general theory of membrane transport from studies of bacteria. *Nature.* 180:134–136. https://doi.org/10.1038/180134a0

Muth, T.R., and S. Schuldiner. 2000. A membrane-embedded glutamate is required for ligand binding to the multidrug transporter EmrE. *EMBO J.* 19:234–240. https://doi.org/10.1093/emboj/19.2.234

Nair, A.V., H. Singh, S. Raturi, A. Neuberger, Z. Tong, N. Ding, K. Agboh, and H.W. van Veen. 2016. Relocation of active site carboxylates in major facilitator superfamily multidrug transporter LmrP reveals plasticity in proton interactions. *Sci. Rep.* 6:38052. https://doi.org/10.1038/srep38052

Newstead, S. 2015. Molecular insights into proton coupled peptide transport in the PTR family of oligopeptide transporters. *Biochim. Biophys. Acta.* 1850:488–499. https://doi.org/10.1016/j.bbagen.2014.05.011

Newstead, S. 2017. Recent advances in understanding proton coupled peptide transport via the POT family. *Curr. Opin. Struct. Biol.* 45:17–24. https://doi.org/10.1016/j.sbi.2016.10.018

Nishizawa, T., S. Kita, A.D. Maturana, N. Furuya, K. Hirata, G. Kasuya, S. Ogasawara, N. Dohmae, T. Iwamoto, R. Ishitani, and O. Nureki. 2013. Structural basis for the counter-transport mechanism of a H+/Ca2+ exchanger. *Science.* 341:168–172. https://doi.org/10.1126/science.1239002

Nomura, N., G. Verdon, H.J. Kang, T. Shimamura, Y. Nomura, Y. Sonoda, S.A. Hussien, A.A. Qureshi, M. Coincon, Y. Sato, et al. 2015. Structure and mechanism of the mammalian fructose transporter GLUT5. *Nature.* 526:397–401. https://doi.org/10.1038/nature14909

Nur, S., and C.E. Adams. 2016. Chlorpromazine versus reserpine for schizophrenia. *Cochrane Database Syst. Rev.* 4:CD012122.

Olivella, M., A. Gonzalez, L. Pardo, and X. Deupi. 2013. Relation between sequence and structure in membrane proteins. *Bioinformatics.* 29:1589–1592. https://doi.org/10.1093/bioinformatics/btt249

Pao, S.S., I.T. Paulsen, and M.H. Saier Jr. 1998. Major facilitator superfamily. *Microbiol. Mol. Biol. Rev.* 62:1–34.

Paulsen, I.T., M.H. Brown, and R.A. Skurray. 1996. Proton-dependent multidrug efflux systems. *Microbiol. Rev.* 60:575–608.

Peter, D., J. Jimenez, Y. Liu, J. Kim, and R.H. Edwards. 1994. The chromaffin granule and synaptic vesicle amine transporters differ in substrate recognition and sensitivity to inhibitors. *J. Biol. Chem.* 269:7231–7237.

Radestock, S., and L.R. Forrest. 2011. The alternating-access mechanism of MFS transporters arises from inverted-topology repeats. *J. Mol. Biol.* 407:698–715. https://doi.org/10.1016/j.jmb.2011.02.008

Rastogi, V.K., and M.E. Girvin. 1999. Structural changes linked to proton translocation by subunit c of the ATP synthase. *Nature.* 402:263–268. https://doi.org/10.1038/46224

Ray, A., E. Lindahl, and B. Wallner. 2010. Model quality assessment for membrane proteins. *Bioinformatics.* 26:3067–3074. https://doi.org/10.1093/bioinformatics/btq581

Reiersen, H., and A.R. Rees. 2001. The hunchback and its neighbours: proline as an environmental modulator. *Trends Biochem. Sci.* 26:679–684. https://doi.org/10.1016/S0968-0004(01)01957-0

Rudnick, G., S.S. Steiner-Mordoch, H. Fishkes, Y. Stern-Bach, and S. Schuldiner. 1990. Energetics of reserpine binding and occlusion by the chromaffin granule biogenic amine transporter. *Biochemistry.* 29:603–608. https://doi.org/10.1021/bi00455a002

Saier, M.H. Jr., J.T. Beatty, A. Goffeau, K.T. Harley, W.H. Heijne, S.C. Huang, D.L. Jack, P.S. Jähn, K. Lew, J. Liu, et al. 1999. The major facilitator superfamily. *J. Mol. Microbiol. Biotechnol.* 1:257–279.

Sansom, M.S., and H. Weinstein. 2000. Hinges, swivels and switches: the role of prolines in signalling via transmembrane alpha-helices. *Trends Pharmacol. Sci.* 21:445–451. https://doi.org/10.1016/S0165-6147(00)01553-4

Scherman, D., and J.P. Henry. 1984. Reserpine binding to bovine chromaffin granule membranes. Characterization and comparison with dihydrotetrabenazine binding. *Mol. Pharmacol.* 25:113–122.

Schuldiner, S. 2014. Competition as a way of life for H(+)-coupled antiporters. *J. Mol. Biol.* 426:2539–2546. https://doi.org/10.1016/j.jmb.2014.05.020

Schuldiner, S., A. Shirvan, and M. Linial. 1995. Vesicular neurotransmitter transporters: from bacteria to humans. *Physiol. Rev.* 75:369–392. https://doi.org/10.1152/physrev.1995.75.2.369

Sigal, N., N. Fluman, S. Siemion, and E. Bibi. 2009. The secondary multidrug/proton antiporter MdfA tolerates displacements of an essential negatively charged side chain. *J. Biol. Chem.* 284:6966–6971. https://doi.org/10.1074/jbc.M808877200

Smirnova, I., V. Kasho, J. Sugihara, and H.R. Kaback. 2011. Opening the periplasmic cavity in lactose permease is the limiting step for sugar binding. *Proc. Natl. Acad. Sci. USA.* 108:15147–15151. https://doi.org/10.1073/pnas.1112157108

Steiner-Mordoch, S., A. Shirvan, and S. Schuldiner. 1996. Modification of the pH profile and tetrabenazine sensitivity of rat VMAT1 by replacement of aspartate 404 with glutamate. *J. Biol. Chem.* 271:13048–13054. https://doi.org/10.1074/jbc.271.22.13048

Stern-Bach, Y., N. Greenberg-Ofrath, I. Flechner, and S. Schuldiner. 1990. Identification and purification of a functional amine transporter from bovine chromaffin granules. *J. Biol. Chem.* 265:3961–3966.

Stitzel, R.E. 1976. The biological fate of reserpine. *Pharmacol. Rev.* 28:179–208.

Sugihara, J., L. Sun, N. Yan, and H.R. Kaback. 2012. Dynamics of the L-fucose/H+ symporter revealed by fluorescence spectroscopy. *Proc. Natl. Acad. Sci. USA.* 109:14847–14851. https://doi.org/10.1073/pnas.1213445109

Sun, L., X. Zeng, C. Yan, X. Sun, X. Gong, Y. Rao, and N. Yan. 2012. Crystal structure of a bacterial homologue of glucose transporters GLUT1-4. *Nature.* 490:361–366. https://doi.org/10.1038/nature11524

Tanaka, Y., C.J. Hipolito, A.D. Maturana, K. Ito, T. Kuroda, T. Higuchi, T. Katoh, H.E. Kato, M. Hattori, K. Kumazaki, et al. 2013. Structural basis for the drug extrusion mechanism by a MATE multidrug transporter. *Nature.* 496:247–251. https://doi.org/10.1038/nature12014

Taniguchi, R., H.E. Kato, J. Font, C.N. Deshpande, M. Wada, K. Ito, R. Ishitani, M. Jormakka, and O. Nureki. 2015. Outward- and inward-facing structures of a putative bacterial transition-metal transporter with homology to ferroportin. *Nat. Commun.* 6:8545. https://doi.org/10.1038/ncomms9545

Tieleman, D.P., I.H. Shrivastava, M.R. Ulmschneider, and M.S. Sansom. 2001. Proline-induced hinges in transmembrane helices: possible roles in ion channel gating. *Proteins.* 44:63–72. https://doi.org/10.1002/prot.1073

Torres, G.E., and S.G. Amara. 2007. Glutamate and monoamine transporters: new visions of form and function. *Curr. Opin. Neurobiol.* 17:304–312. https://doi.org/10.1016/j.conb.2007.05.002

Ugolev, Y., T. Segal, D. Yaffe, Y. Gros, and S. Schuldiner. 2013. Identification of conformationally sensitive residues essential for inhibition of vesicular monoamine transport by the noncompetitive inhibitor tetrabenazine. *J. Biol. Chem.* 288:32160–32171. https://doi.org/10.1074/jbc.M113.502971

Vardy, E., I.T. Arkin, K.E. Gottschalk, H.R. Kaback, and S. Schuldiner. 2004. Structural conservation in the major facilitator superfamily as revealed by comparative modeling. *Protein Sci.* 13:1832–1840. https://doi.org/10.1110/ps.04657704

Vardy, E., S. Steiner-Mordoch, and S. Schuldiner. 2005. Characterization of bacterial drug antiporters homologous to mammalian neurotransmitter transporters. *J. Bacteriol.* 187:7518–7525. https://doi.org/10.1128/JB.187.21.7518-7525.2005

von Heijne, G. 1991. Proline kinks in transmembrane alpha-helices. *J. Mol. Biol.* 218:499–503. https://doi.org/10.1016/0022-2836(91)90695-3

Waight, A.B., B.P. Pedersen, A. Schlessinger, M. Bonomi, B.H. Chau, Z. Roe-Zurz, A.J. Risenmay, A. Sali, and R.M. Stroud. 2013. Structural basis for alternating access of a eukaryotic calcium/proton exchanger. *Nature.* 499:107–110. https://doi.org/10.1038/nature12233

Weaver, J.A., and J.D. Deupree. 1982. Conditions required for reserpine binding to the catecholamine transporter on chromaffin granule ghosts. *Eur. J. Pharmacol.* 80:437–438. https://doi.org/10.1016/0014-2999(82)90093-0

Weihe, E., and L.E. Eiden. 2000. Chemical neuroanatomy of the vesicular amine transporters. *FASEB J.* 14:2435–2449. https://doi.org/10.1096/fj.00-0202rev

Weinglass, A.B., I.N. Smirnova, and H.R. Kaback. 2001. Engineering conformational flexibility in the lactose permease of Escherichia coli: use of glycine-scanning mutagenesis to rescue mutant Glu325-->Asp. *Biochemistry.* 40:769–776. https://doi.org/10.1021/bi002171m

Wisedchaisri, G., M.-S. Park, M.G. Iadanza, H. Zheng, and T. Gonen. 2014. Proton-coupled sugar transport in the prototypical major facilitator superfamily protein XylE. *Nat. Commun.* 5:4521. https://doi.org/10.1038/ncomms5521

Yaffe, D., S. Radestock, Y. Shuster, L.R. Forrest, and S. Schuldiner. 2013. Identification of molecular hinge points mediating alternating access in the vesicular monoamine transporter VMAT2. *Proc. Natl. Acad. Sci. USA.* 110:E1332–E1341. https://doi.org/10.1073/pnas.1220497110

Yaffe, D., A. Vergara-Jaque, Y. Shuster, D. Listov, S. Meena, S.K. Singh, L.R. Forrest, and S. Schuldiner. 2014. Functionally important carboxyls in a bacterial homologue of the vesicular monoamine transporter (VMAT). *J. Biol. Chem.* 289:34229–34240. https://doi.org/10.1074/jbc.M114.607366

Yaffe, D., A. Vergara-Jaque, L.R. Forrest, and S. Schuldiner. 2016. Emulating proton-induced conformational changes in the vesicular monoamine transporter VMAT2 by mutagenesis. *Proc. Natl. Acad. Sci. USA.* 113:E7390–E7398. https://doi.org/10.1073/pnas.1605162113

Yan, N. 2015. Structural Biology of the Major Facilitator Superfamily Transporters. *Annu. Rev. Biophys.* 44:257–283. https://doi.org/10.1146/annurev-biophys-060414-033901

Yelin, R., and S. Schuldiner. 1995. The pharmacological profile of the vesicular monoamine transporter resembles that of multidrug transporters. *FEBS Lett.* 377:201–207. https://doi.org/10.1016/0014-5793(95)01346-6

Zheng, H., G. Wisedchaisri, and T. Gonen. 2013. Crystal structure of a nitrate/nitrite exchanger. *Nature.* 497:647–651. https://doi.org/10.1038/nature12139

Zhou, Y., L. Guan, J.A. Freites, and H.R. Kaback. 2008. Opening and closing of the periplasmic gate in lactose permease. *Proc. Natl. Acad. Sci. USA.* 105:3774–3778. https://doi.org/10.1073/pnas.0800825105

Zhou, Y., Y. Nie, and H.R. Kaback. 2009. Residues gating the periplasmic pathway of LacY. *J. Mol. Biol.* 394:219–225. https://doi.org/10.1016/j.jmb.2009.09.043